SHIP SCALE VALIDATION OF CFD MODEL OF SELF-PROPELLED SHIP

HENRIK MIKKELSEN*, MADS L. STEFFENSEN*, COSMIN CIORTAN† AND JENS H. WALTHER*‡

*Technical University of Denmark (DTU)
Department of Mechanical Engineering
Nils Koppels Allé, Building 404, 2700 Kgs. Lyngby, Denmark.
e-mail: jhw@mek.dtu.dk, web page: http://www.mek.dtu.dk/

† DNV-GL
Section for Hydrodynamic and Stability
Veritasveien 1, 1363 Høvik, Norway

‡ Swiss Federal Institute of Technology Zurich
Computational Science & Engineering Laboratory
Clausiusstrasse 33, CH-8092 Switzerland

Key words: Computational fluid dynamics, Ship scale ship propulsion, Sea trial validation, Self-propulsion simulation

Abstract. This paper presents a comparison of towing tank testing, ship scale computational fluid dynamics (CFD) simulations, sea trial measurements and in-service performance. The study includes extensive convergence tests and validation of both resistance, open-water and self-propulsion CFD simulations in both model and ship scale. The self-propulsion CFD simulations are conducted using a novel method. This method includes calculating the wave-making resistance separately, in order to reduce the computational cost.

The results of the ship scale self-propulsion CFD show an average overestimation of delivered power of 2 % compared to the sea trial results, where the predicted delivered power using the towing tank approach shows an average overestimation of delivered power of 6 %. Both predictions are within the uncertainty of the speed trial measurements. The study shows that both the towing tank approach and ship scale CFD can make reasonable and similar estimations of the ship scale performance of a ship. Furthermore, we find that for the present ship, CFD is able to predict performance as accurately as towing tank procedures, indicating that ship scale CFD is a mature tool for use in future ship designs.

1 INTRODUCTION

Traditionally, the performance of a ship design is estimated by conducting towing tank tests on a downscaled version of the ship (model scale). The results from these towing tank tests are then extrapolated to the scale of the actual ship (ship scale). An alternative to testing in a towing tank is to simulate the flow around the ship using computational fluid dynamics (CFD). CFD simulations can be performed in ship scale, which eliminates scale effects and the need for extrapolation. A disadvantage of using CFD is modelling errors which occur due to simplification of the flow physics (e.g. turbulence).

Extensive validation of CFD simulations in model scale has been conducted by e.g [7], which showed good agreement with experimental results of the research ship Kriso Container Ship (KCS). Furthermore, validation workshops have been hosted, where the participants blindly submit CFD results to be compared with towing tank results [9, 8].

With the increased confidence in model scale, the next step is ship scale CFD, which has been studied by e.g. [1]. However, in ship scale publicly accessible validation data is extremely rare. The largest contribution so far on ship scale validation, is the Lloyd's Register workshop from 2016 [11]. A comparison between ship scale CFD and sea trial measurements of a car carrier has been conducted by [6] showing accurate correspondence.

The present paper includes a comparison between sea trial measurements, ship scale CFD, model tank experiments and in-service performance. It is the first published study, where all these elements are compared. The conducted self-propulsion CFD simulations in the present study calculate the wave-making resistance in a different way than e.g. [13, 6] since the wave-making resistance is calculated separately. This results in a significantly reduced computational cost.

The key to a useful comparison is highly accurate sea trial data. Sea trial data generally has significant uncertainties because of the lack of control in the experimental environment. There is a focus in the industry on obtaining increasingly accurate sea trial results, as seen with introduction of the new sea trial procedure ISO 15016:2015 cf. [4]. Besides the difficulties in conducting experiments at such a large scale, it is also important to remember that there are many stakeholders in a sea trial, each with different interests.

2 THE STUDIED VESSEL AND MEASUREMENTS

The ship considered in the present study is a $L_{\mathrm{PP}} = 196\,\mathrm{m}$ bulk carrier built by a Japanese shipyard.

2.1 Hull

The hull has been provided as a 3D geometry by the Japanese shipyard. The hull and water lines of the design and sea trial conditions are shown in Figure 1. The displacement of the ship in sea trial condition is 40.2 % of the displacement in the design condition. The vessel is at design speed sailing at a Reynolds number $\mathrm{Re} = \frac{V_{\mathrm{Design}} L_{\mathrm{PP}}}{\nu} \approx 1.1 \times 10^9$ and a Froude number $\mathrm{Fr} = \frac{V_{\mathrm{Design}}}{\sqrt{g L_{\mathrm{PP}}}} \approx 0.2$.

2.2 Propeller

The data of the actual and the stock propeller can be seen in Table 1. Due to confidentiality it has not been possible for the propeller manufacturer to provide the 3D geometry of the actual propeller. Therefore, the stock propeller has been used for all CFD simulations.

Figure 1: Hull geometry. The upper horizontal line is the water line of the design condition, and the lower horizontal line is the water line of the sea trial condition. Seen from starboard side.

Parameter	Actual	Stock
Ship scale diameter	6.00 m	6.00 m
Boss ratio	0.1417	0.18
Pitch ratio (0.7r)	0.7284	0.76
Expanded area ratio	0.48	0.58
Number of blades	4	4

Table 1: Data of the actual and the stock propeller.

2.3 Appendages

The actual ship is mounted with a rudder, a number of upstream stator fins and bilge keels. The "to-be-built" 2D-drawings of the stator fins and rudder including rudder bulb have been provided by the Japanese shipyard. Based on these drawings, the stator fins and rudder geometry have been recreated in 3D.

The stator fins are a retrofitted energy saving device and are mounted upstream of the propeller to produce pre-swirl.

Bilge keels are not included in the CFD simulations since they are not mounted on the model ship in the towing tank test. They are instead accounted for in the towing tank and CFD simulations by using the standard International Towing Tank Committee (ITTC) method [5].

2.4 Towing tank testing

Towing tank tests of the vessel are conducted by the National Maritime Research Institute in Tokyo, Japan. The tests conducted by the towing tank are resistance tests, open water tests and self-propulsion tests. The results from the towing tank have been extrapolated using the standard ITTC extrapolation procedure [5].

2.5 Sea trial

Four sister vessels of the same design have been built in total. Speed trials have been conducted for each of the four sister ships. In 2015, the International Maritime Organisation (IMO) and ITTC released ISO15016:2015 [4], an updated version of the ISO 15016:2002 standard procedure for carrying out and correcting speed trials. The speed trials of the fourth ship have been conducted mostly as described in [4]. The speed trials of the three other ships have been conducted prior to the release of that procedure, but is assumed to have been conducted using similar procedures. The Japanese shipyard has provided the results of these speed trials for all four ships. The main measurements in the speed trial are speed, propeller rate of rotation, and the engine power. After the speed trial, the measurements are corrected for the environment forces.

2.5.1 Speed measurement and corrections

The speed of the ship during the speed trial is measured using a Differential-GPS (DGPS). The temporary DGPS is installed on top of the bridge and is connected to a laptop. From the DGPS data, the ship speed over ground is calculated by assuming no lateral drift. The ship speed is recorded during each speed run, with a sampling frequency of about 1 Hz. From the recorded data, a mean ship speed is calculated.

The speed over ground signal is visually inspected, showing only minor fluctuation. Based on observations, it is concluded that the speed signal is reliable and that the mean is an accurate measurement of the actual speed over ground of the ship. To obtain the speed through water, the speed measurement has to be corrected for current. The measured speed is corrected for the tidal current by using double runs: one in the direction against the current and one with the current.

2.5.2 Power measurement and correction

The power of the engine is calculated from the engine rate of rotation and the the fuel index (FI), which is indicating the amount of fuel injected ranging from 0 to 100, using the following formula provided by the engine manufacturer:

$$P = C_{cyl}\, C_{eng}\, n\, p_{me} \tag{1}$$

$$C_{eng} = \frac{60}{2\pi}\, 100.7355 \times 10^{-3} \tag{2}$$

$$p_{me} = 19375\, FI - 105938 \tag{3}$$

Here P denotes the engine power in Watts, C_{cyl} and C_{eng} are cylinder coefficient provided by the engine manufacturer, n is the rate of revolutions per second, p_{me} is the mean effective pressure in Pascals. The mean effective pressure (p_{me}) is calculated from the fuel index cf. Equation (3) as provided by the engine manufacturer:

Both the rate of rotation and the fuel index are sampled directly from the engine control system. The revolutions per minute of the engine is measured directly on the shaft, and there is no gear box.

ISO15016:2015 [4] states that the power has to be measured using a torque meter mounted directly on a shaft. Such a device is also installed, but the measurements are not used in the speed trial results.

The measured power is corrected for the difference between the planned and the actual displacement of the ship [4]. The planned displacement of the ship in sea trial condition is calculated before conducting the sea trial, and the actual displacement is measured at the beginning of the sea trial. The correction is conducted by the shipyard. The difference in displacements is less than 1 %.

The performance of the ship is corrected for the added wind resistance [4, Annex C]. The wind correction is based on an estimated drag coefficient, an estimated projected front area and

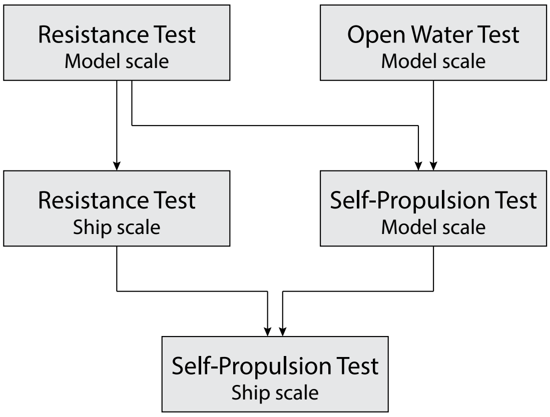

Figure 2: The five CFD setups. The arrows indicate the direction of the work flow.

a relative wind speed. The absolute wind speed is measured using a wind anemometer placed above the bridge.

The results used in the present study are corrected for waves as described in [4]. The method requires significant wave height and direction of the waves. These two parameters were not recorded during any of the sea trials of the four sister ships. Instead, the parameters have been estimated using Atmospheric Reanalysis (ERA)-Interim data from satellite weather data and a meteorological model.

3 COMPUTATIONAL FLUID DYNAMICS

This section briefly describes the CFD setups developed and used in this study. More details can be found in [10]. All the CFD simulations are performed by discretizing the domain by hexahedral cells in the commercial CFD-code STAR-CCM+ v.10.04.011 from CD-Adapco, now SIEMENS [2]. STAR-CCM+ discretizes the governing equations using an unstructured finite-volume method. The code is widely used in the marine industry and is well-known for its capabilities within marine applications.

In total five CFD setups are developed: model scale resistance setup, ship scale resistance setup, model scale open water setup, model scale self-propulsion setup, and ship scale self-propulsion setup. The five CFD setups are illustrated Figure 2.

3.1 Governing equations and CFD output

The governing equations of an incompressible Newtonian fluid are the continuity and Navier-Stokes equations:

$$\frac{\partial u_i}{\partial x_i} = 0 \tag{4}$$

$$\rho \frac{\partial u_i}{\partial t} + \rho u_j \frac{\partial u_i}{\partial x_j} = -\frac{\partial p}{\partial x_i} + \frac{\partial}{\partial x_j}\left(2\mu S_{ij} - \rho \overline{u_j' u_i'}\right) \tag{5}$$

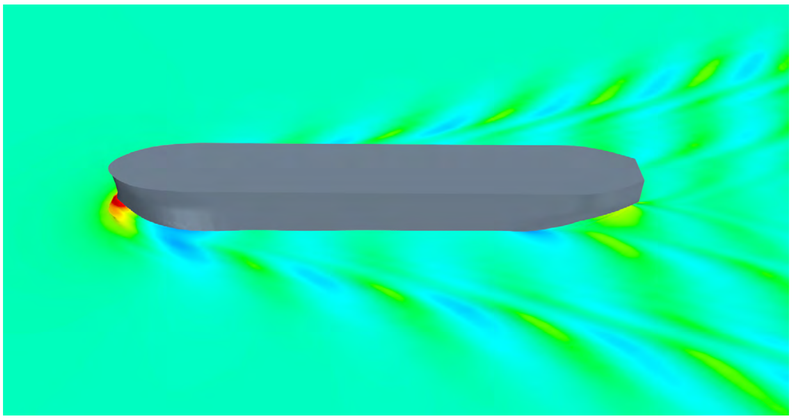

Figure 3: Wave elevation from model scale resistance simulation.

where u_i is the velocity vector, t is time, p is pressure, μ is dynamic viscosity, $S_{ij} = \frac{1}{2}\left(\frac{\partial u_i}{\partial x_j} + \frac{\partial u_j}{\partial x_i}\right)$ is the mean strain rate and u' is the fluctuating part of the velocity.

The calm free surface in the resistance and self-propulsion simulations is resolved using the volume of fluid (VOF) method in STAR-CCM+ [2, 3]. The turbulence is modelled using the realisable k-ϵ turbulence model [2, 12].

One output from the CFD simulations is the total ship resistance, which is calculated by integrating the shear and pressure force on the entire ship hull excluding the propeller.

The propeller thrust T is calculated by integrating all shear and pressure forces on the propeller parallel to the shaft axis.

The propeller torque Q is calculated by integrating all moment contribution from both the shear and pressure forces on the propeller around the shaft axis.

3.2 CFD resistance test

The calm water resistance calculation is first created in model scale and validated by comparing results with the towing tank results. The validated model scale setup is then scaled up to a ship scale setup. Convergence studies are conducted in both the model and ship scale setup. Results of the ship scale CFD setup are compared with the extrapolated resistance data from the towing tank data. More details on the CFD resistance setup, can be found in [10].

All resistance simulations are performed in the sea trial condition similarly to the towing tank test and sea trial. The initial CFD setup used to estimate the calm water resistance is an automated CFD setup developed by OSK-ShipTech A/S. An illustration of the wave elevation in a resistance simulation is shown in Figure 3.

The CFD resistance setup uses a number of different physics models to describe the flow around the ship. Free surface waves are modelled using volume of fluid [2, 3]. The hull is allowed dynamic pitch and heave motions. The simulations are solved using a 1st order implicit unsteady solver.

After demonstrating good agreement with the towing tank results, the ship scale resistance setup is created by scaling up the model scale resistance setup with the scaling factor. The prism layers is changed so the wall y$^+$ is still mostly in the range of 50–100.

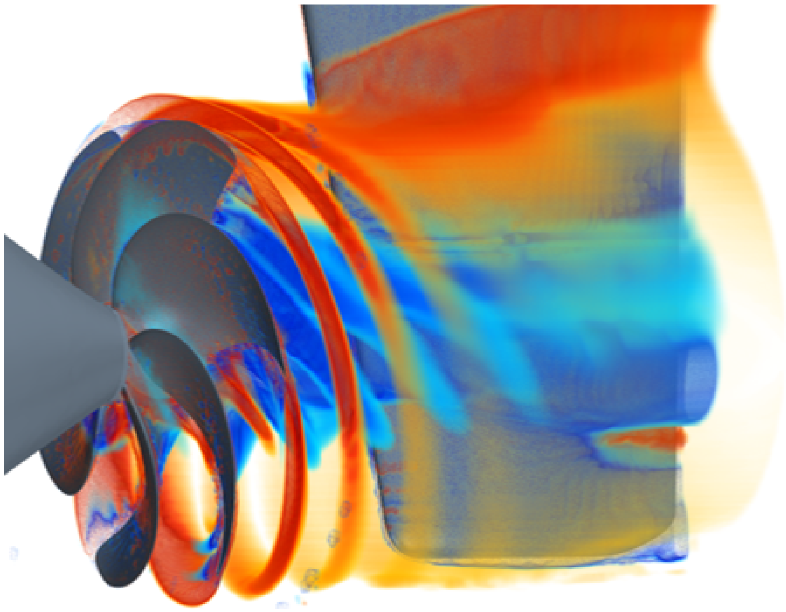

Figure 4: Vorticity downstream of propeller in self-propulsion simulation.

3.3 CFD open water

Modelling the open water test using CFD is less complex than modelling the self-propulsion test because the hull-propeller interaction is not included in the open water setup. The idea is that a separately validated resistance and open water setup can be combined to a self-propulsion setup by using the validated mesh and time step settings. This self-propulsion setup can then be validated in model scale by comparing it with self-propulsion results from towing tank tests.

The single phase open-water CFD setup is fully resolving the boundary layer with wall y+ values approximately equal to one.

The open water setup uses two domains: A stationary domain and a rotating domain. The two domains are connected by an interface. The shape of the stationary domain is a rectangular cuboid. The shape of the rotating domain is a cylinder which is located inside the static domain and around the propeller. In order to better resolve the flow around the propeller, two refinement zones are used to refine the mesh in the volume around the propeller.

The propeller movement can be modelled using two methods: the moving reference frame (MRF) method or the sliding mesh (SM) method. For the open-water simulation, MRF is used.

3.4 CFD self-propulsion

The self-propulsion CFD setup is created by combining the model scale resistance CFD setup with the propeller and the open water CFD setup. As in the open water setup, the self-propulsion setup uses two domains; a large static domain, with a small rotating domain inside. The shape of the static domain is a rectangular cuboid, and the shape of the rotating domain is a cylinder. The resolved flow around propeller is illustrated in Figure 4.

In order to minimize computational cost, the free surface is not included directly in the self-propulsion simulation. This in conducted by replacing the free surface with a slip wall. The method is originally developed and validated at DNV-GL. Instead of modelling the dynamic pitch and heave using the DFBI model, the dynamic pitch and heave of the resistance simulations are prescribed to the self-propulsion simulations before they are simulated. Removing the free surface waves from the simulations gives rise to another problem. In reality, a stern wave is created by the ship. The stern wave increases the water height above the propeller, which affects the flow. In order to resolve this, the symmetry plane is raised to a highest point of the stern wave obtained in the resistance simulation. In the present case, the symmetry plane is elevated 3 % of the draft in the sea trial condition. The decision not to model the free surface waves and to raise the calm water surface decreases the measured resistance on the ship. In order to compensate for this change, a free surface correction is performed on the results of the self-propulsion simulations. The correction is performed in two steps. The first step is to correct for not modelling the free surface waves, which reduces the hull resistance by removing the wave making resistance. The wave making resistance is quantified by simulating the resistance setup both with and without the free surface waves. The difference between those two results is the wave making resistance:

$$R_W = R_T - R_V \tag{6}$$

where R_W is the wave making resistance, R_T is the total resistance and R_V is the total resistance without free surface waves, also referred to as the viscous resistance. In the present study the wave making resistance is approximately 25 % of the total resistance.

The second step is to correct for the raised free surface which increases the resistance on the hull, because a larger surface area is submerged. The increase in resistance is quantified by simulating the resistance both with the initial and the raised surface heights without modelling the free surface. The difference between those two results is the added resistance due to the raised surface ΔR_{SH}, which in the present study is approximately 7 % of the total resistance, is given by:

$$\Delta R_{SH} = R_{V,SH} - R_V \tag{7}$$

where $R_{V,SH}$ is the viscous resistance with the raised surface height. The resistance of the self-propulsion simulations can then be corrected for wave making resistance and added resistance due to the raised surface height:

$$R_{Tm} = R_{Vm,SH} + R_{Wm} - \Delta R_{SHm} \tag{8}$$

where the subscript 'm' refers to model scale.

For the self-propulsion simulations a combination of the two methods is used for increased computational efficiency. The modelling of the propeller rotation is initialized by using the MRF method, followed by the SM method. The SM uses a time step corresponding to two degrees of propeller rotation. These steps with different methods and time steps are used to minimize the computational cost. One advantage of using the method with the separate calculation of the wave-making resistance is that the MRF step can be solved with a steady-state solver. Furthermore, it is not necessary to solve the volume fraction transport equation or to refine

Simulation type	Parameter	Discrepancy from model tank test
Resistance	Total resistance	≈ 0–2 %
Open water	Thrust coefficient	≈ 1–3 %
	Torque coefficient	≈ 3–5 %
	Efficiency	≈ 2–7 %
Self-propulsion	Thrust coefficient	≈ 3–7 %
	Torque coefficient	≈ 6–7 %
	Rotation rate	≈ 2–6 %

Table 2: Discrepancy of model scale CFD results from model tank test [10].

the mesh near the free surface. This significantly decreases the computational cost. The self-propulsion simulation has more than double as many cells as the resistance simulation and a time step in the SM step, which is approximately a factor of 30 smaller cf. [10]. However, the computational cost of the self-propulsion simulation, using the present approach, is only approximately 20 % higher than a resistance simulation.

The CFD self-propulsion setup is carried out by changing the rate of revolution of the propeller until a force equilibrium is obtained in the sailing direction within a reasonable small tolerance.

The ship scale self-propulsion setup is created by scaling up the model scale self-propulsion setup according to the scaling factor. The prism layers is changed so the wall y^+ is still mostly in the range of 30–100 on the hull and propeller.

The free surface correction method is changed slightly from model scale to ship scale in order to account for the roughness resistance, air resistance and bilge keel resistance which are only relevant for the ship scale simulations. The wave making resistance and the added resistance of the increased surface height are calculated similarly to Equations (6) and (7).

The ship scale resistance is then calculated using:

$$R_{Ts} = \frac{S + S_{BK}}{S}(R_{Vs,SH} + \Delta R_F) + R_{Ws} + R_{AAS} - \Delta R_{SHs} \tag{9}$$

where the subscript 's' refers to ship scale, S is the wetted surface without the bilge keels, S_{BK} is the wetted surface including the bilge keels, ΔR_F is the roughness resistance, and R_{AAS} is the air resistance. The correlation allowance C_A cf. [5] is not included in the total resistance because its purpose is to correct for systematic errors in the towing tank extrapolation procedure.

4 RESULTS AND DISCUSSION

4.1 Validation of the CFD simulations

It is essential to ensure the accuracy of the CFD setup before conclusions are based on the results of the setup.

Convergence studies have been conducted for both the spatial and temporal discretization for all five setups. The discrepancy of the model scale CFD results from the model tank test are shown in Table 2. More details can be found in [10].

Based on the convergence studies and comparisons to the towing tank tests, the results of the model scale self-propulsion setup are reasonable. The ship scale set-up has been built up in the same way as the model scale CFD set-up. All convergence tests and comparisons in ship scale have shown satisfactory results cf. [10].

4.2 Comparison of sea trial and in-service performance data

The results provided by the shipyard are the measured values corrected for wind and current. The procedures of the sea trial and corrections are briefly described in Section 2.5.

The results from the sea trials seen in Figure 5 show high correlation between speed and power, and low scatter of the data points. This indicates that the accuracy of the speed trial data is high. However, systematic errors can not be determined solely from the data provided for this study.

The correction for wind, waves and current is a possible sources for systematic errors. As mentioned, the ISO 15016:2015 procedure [4] defines strict standards for conducting sea trials and ensures accurate measurements and corrections. The power measurements based on engine formulas are another possible source for systematic errors.

A way to validate the results from the sea trial is by comparing the results with performance measurements on the ship after the delivery while it is in service. The ship owner has provided in-service performance data in sea trial condition corrected for wind and waves by the ship owner. The data is the mean performance of all four sister ships in the first 3-9 months of operation. The power is based on torque measurements directly on the shaft and not the engine manufacturer formula as in case of the sea trial measurements. The ship owner has estimated the uncertainty to be approximately $\pm 3.5\,\%$ maximum continuous rating (MCR). Uncertainties in the performance data includes e.g. uncertainties in the raw torque measurement, the correction for wind and waves and the averaging of the data from the four sister ships.

The results of the sea trial are compared to the in-service performance data in Figure 5. The comparison shows that the ships use more power in-service than during sea trial. On average, the sea trial data shows $8\,\%$ less power than the in-service performance data. This is expected since the ships are in excellent condition at the sea trial with minimal fouling on the ship hull. Even though both the sea trial data and the in-service performance data have uncertainties, the relatively low offset in power shows that the sea trial data and the in-service performance data measures delivered power in the same range. Furthermore, there is only a small scatter of the sea trial data, which indicates good consistency in the measurements.

4.3 Comparison of sea trial, CFD and towing tank test

The sea trial results presented in Section 4.2 are compared to the extrapolated self-propulsion results from the towing tank test and ship scale CFD in Figure 5. In this comparison, it is assumed that there is no loss in the shaft, which is a reasonable assumption, since there is no gear.

The extrapolated towing tank results are overestimating the power by approximately 3–9 % with an average of 6 % compared to the sea trial results. Considering that towing tank tests are conducted at a much lower Reynolds number and extrapolated, the observed discrepancies are satisfactory.

Is it important to remember that the extrapolation of the towing tank results are performed by the authors using the standard ITTC procedure [5]. Based on the authors' experience, many

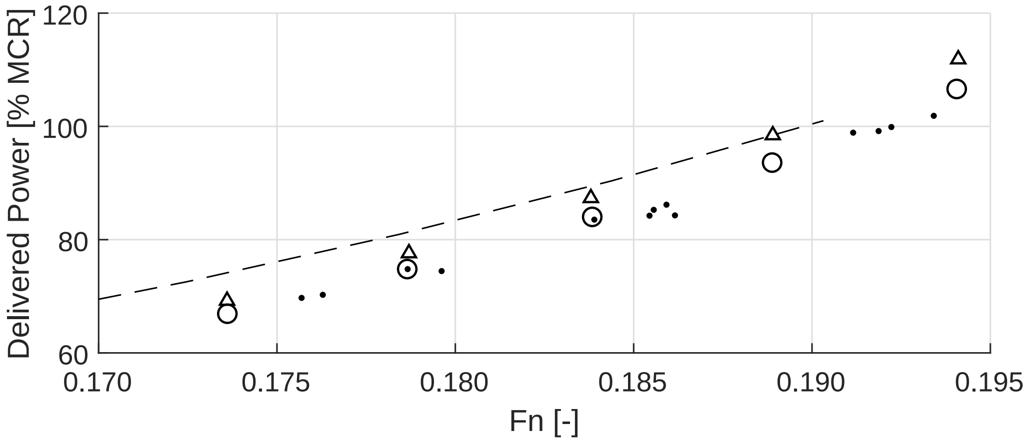

Figure 5: Comparison of the corrected speed trial results (dot), the extrapolated self-propulsion results (triangle) from the towing tank and the ship scale CFD self-propulsion results (circle). Delivered power P_{Ds} as a function of Froude number Fn.

towing tanks use slightly different coefficients and corrections than the standard ITTC procedure recommends. These changes to the standard procedure are based on experience, tradition, studies of systematic errors and validation studies of each tank. It has not been possible to have the exact extrapolation procedure that the towing tank uses in the present study. Therefore, the extrapolation procedure used in this study is the standard ITTC procedure.

Furthermore, it can be seen in Figure 5 that the CFD overestimates the delivered power by approximately 0–5 % with an average of 2 %. It is important to remember that the CFD simulations are performed using the stock propeller and not the actual propeller.

5 CONCLUSION

A ship scale self-propulsion CFD setup using a new method developed by DNV-GL has been built and validated. The results of the CFD simulations showed an overestimation of the delivered power by approximately 2 % on average compared to the sea trial results. Raw experimental towing tank test results have been extrapolated to ship scale using the ITTC procedure. It was found that this prediction overestimated the delivered power with 6 % in average compared to the sea trial results. Both predictions are within the uncertainty of the speed trial measurements.

6 ACKNOWLEDGEMENT

The research was supported by The Danish Maritime Fund under grant 2015-103 and 2018-11, whose support is greatly appreciated.

Furthermore, we would like to express our sincere gratitude to the Japanese shipyard and European ship-owner for inviting us to the sea trial and providing unique and rarely shared data.

REFERENCES

[1] A. M. Castro, P. M. Carrica, and F. Stern. Full scale self-propulsion computations using discretized propeller for the KRISO container ship KCS. *Comput. Fluids*, 51(1):35–47, 2011.

[2] CD-Adapco. STAR-CCM+ Documentation, Version 10.04, 2015.

[3] C. Hirt and B. Nichols. Volume of fluid (VOF) method for the dynamics of free boundaries. *J. Comput. Phys.*, 39(1):201–225, 1981.

[4] IMO. ISO 15016:2015. *MEPC 68/INF.14*, 2015.

[5] ITTC. Recommended Procedures and Guidelines, 1978 ITTC Performance Prediction Method, 2005.

[6] H. Jasak, V. Vukčević, I. Gatin, and I. Lalović. CFD validation and grid sensitivity studies of full scale ship self propulsion. *Int. J. Nav. Archit. Ocean Eng.*, 2018.

[7] J. Kim, I.-R. Park, K.-S. Kim, and S.-H. Van. Numerical Simulation of Turbulent Free Surface Flow around a Self-Propelled Ship. In *Proc. Fifteenth Int. Offshore Polar Eng. Conf.*, pages 180–186, Seoul, Korea, 2005.

[8] L. Larsson, F. Stern, M. Visonneau, T. Hino, N. Hirata, and J. Kim. *PROCEEDINGS, TOKYO 2015 WORKSHOP ON CFD IN SHIP HYDRODYNAMICS*. 2015.

[9] L. Larsson, F. Stern, and M. Vsonneau. Gothenburg 2010 A Workshop on Numerical Ship Hydrodynamics Editors. II(1652), 2010.

[10] H. Mikkelsen and M. L. Steffensen. *Full Scale Validation of CFD Model of Self-Propelled Ship*. Master's thesis, Technical University of Denmark, https://doi.org/10.13140/RG.2.2.25689.21607, 2016.

[11] D. Ponkratov. 2016 Workshop on Ship Scale Hydrodynamic Computer Simulation. Lloyd's Register, 2017.

[12] T.-H. Shih, W. W. Liou, A. Shabbir, Z. Yang, and J. Zhu. A new k-ϵ eddy viscosity model for high Reynolds number turbulent flows. *Comput. Fluids*, 24(3):227–238, 1995.

[13] C. Zegos and D. Ponkratov. Ship scale CFD free sink, trim & surge self-propulsion simulation and direct comparison to sea trials. *Rina, R. Inst. Nav. Archit. - Int. Conf. Comput. Appl. Shipbuild.*, 2:49–57, 2015.